Wireless Pers Commun (2012) 67:631–645
DOI 10.1007/s11277-011-0401-9

Downlink System Capacity Analysis in Distributed Antenna Systems

Jun-Bo Wang · Jin-Yuan Wang · Ming Chen

Published online: 13 September 2011

Abstract This paper focuses on the downlink system capacity in distributed antenna systems (DAS). Due to the complexity of actual wireless environments, a composite channel model is established which takes into account three factors, i.e., path loss, lognormal shadowing and Rayleigh fading. Based on the channel model, the probability density function (PDF) of the output signal-to-noise ratio (SNR) is derived. To facilitate the analysis, the distribution of the output SNR is approximated by a lognormal distribution. After that, by making use of selective diversity (SD) scheme for distributed antennas, an approximate analytical expression of the capacity for a mobile station (MS) over a given position is derived. Furthermore, considering the distribution of MSs in the system, a closed-form expression of the system capacity is obtained. Numerical results show that the closed-form expression can evaluate the system capacity performance of DAS very accurately.

Keywords Distributed antenna systems · System capacity · Selective diversity · Composite channel

J.-B. Wang (✉)
Key Laboratory for Information System Security of Ministry of Education, School of Software, Tsinghua University, Beijing 100084, China
e-mail: jbwang@nuaa.edu.cn

J.-B. Wang
State Key Laboratory of Integrated Services Networks, Xidian University, Xi'an 710071, China

J.-B. Wang · J.-Y. Wang
College of Electronic and Information Engineering, Nanjing University of Aeronautics and Astronautics, Nanjing 210016, China

M. Chen
National Mobile Communications Research Laboratory, Southeast University, Nanjing 210096, China

1 Introduction

The next generation wireless communication system will provide very high data rate and mass wireless access service for broad area coverage. However, the conflict between scarce spectrum resources and diversified user demands becomes more and more prominent. The conventional cellular communication system emphasizes the use of low power radio technology to achieve high performances through massive frequency reuse [1]. However, a large number of expensive base stations, complex network planning and frequent handoffs are needed, which lead to high cost and unstable system performances [1]. Therefore, the traditional cellular system is far short of promising the full potentialities which are needed to ensure high capacity, large coverage, good quality of service (QoS), low cost wireless terminals and inexpensive base stations [2–4]. In order to solve these problems, extensive and in-depth studies have been carried out. Recently, the distributed antenna system (DAS) has been drawn much attention because of its potentials in enhancing system performances. Unlike the traditional cellular communication system, the basic idea of DAS is that the distributed antennas are geographically separated from each other. Recent academic studies have shown that the DAS has potential advantages in capacity, power consumption, coverage and outage probability [5–8]. Without any doubt, the DAS can enhance system performances significantly and will become a very promising candidate in future wireless communication system.

System capacity plays an important role in wireless communication systems, and it is of great value to network planning and antenna layout. Up to now, some studies have been done to analyze the capacity performance of DAS. Assuming that the path loss in the system is a constant (0 dB), both the uplink capacity and the downlink capacity of DAS were investigated in [9]. Generally speaking, this is not always so in real systems, because the distance from the base station (BS) to each distributed antenna is usually different. Therefore, path loss can't be ignored. The authors in [1] and [10] also studied the capacity performance of DAS, but the lognormal shadowing was ignored. Due to the large space among distributed antennas, it's not reasonable to assume all the antennas experience the same lognormal shadowing, so the derived theoretical expressions lack generality and can't be applied to evaluate the capacity performance under various scenarios. In [11], the channel gain combines the fast fading, path loss and lognormal shadowing effects, and then an approximate capacity expression is derived using approximation distributions. In addition, we analyzed the downlink capacity of DAS over shadowed Nakagami-m fading channels in [12], and also obtained an expression of capacity. It should be noted that the expression of capacity in [11] or [12] is a function of the position of MS, i.e., given a specific position of the MS, a corresponding capacity can be obtained. Theoretically, the system capacity also relates to the distribution of mobile stations (MSs) in the cell [13]. So far, to the best of the authors' knowledge, the system capacity of DAS has not been completely discussed in open literatures. Therefore, it is of great interest and necessary to study these problems.

Motivated by the researches in [12] and [13], this paper further investigates the downlink system capacity in DAS with selective diversity (SD) scheme. Considering the complexity of actual wireless propagation environment, this paper establishes a composite channel model which takes into account three factors such as path loss, lognormal shadowing and Rayleigh fading. Then, the probability density function (PDF) of the output signal-to-noise ratio (SNR) is derived. To facilitate the theoretical analysis, the distribution of output SNR is approximated by a lognormal distribution. After that, by making use of selective diversity (SD) scheme for distributed antennas, an approximate analytical expression of the capacity for a mobile

station (MS) over a given position is derived. Furthermore, considering the distribution of MSs in the system, a closed-form expression of the system capacity is obtained.

The remainder of this paper is organized as follows: The system model of downlink DAS is described in Section 2. Section 3 analyzes the downlink system capacity, and an approximate distribution of the output SNR is derived. Furthermore, the closed-form expression of system capacity is derived. Numerical results are presented in Section 4 before conclusions are drawn in Section 5.

2 System Model

Consider a single cell distributed antenna system, as shown in Fig. 1. Assume that the radius of the circular cell is R. The BS (also named as DA0) is in the center of the cell, and the distributed antennas are distributed arbitrarily in the cell, which can be denoted as DAi ($i = 1, 2, \cdots, N$). Each distributed antenna is connected to the BS via dedicated wires, fiber optics, or an exclusive RF link. Furthermore, the MSs are also assumed to be randomly distributed in the cell. Due to the implementation limitation, only one single antenna is available at each MS. Without loss of generality, the positions of the MS and DAi are denoted by the polar coordinates (ρ, θ) and (D_i, θ_i), respectively. Note that ρ and θ are the distance and angle of the MS relative to the cell center, while D_i and θ_i are the distance and angle of DAi to the cell center.

This paper only considers the system capacity of the downlink DAS. Mathematically, for the MS located at (ρ, θ) , the received downlink signal from DAi can be expressed as

$$y_i = \sqrt{E} h_i x + z \in \mathbb{C}\ ,\ \forall i \in \{0, 1, 2, \cdots, N\} \tag{1}$$

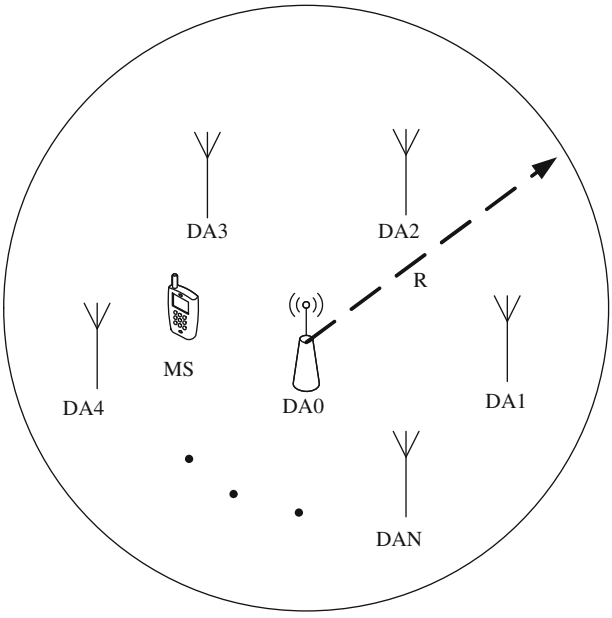

Fig. 1 A distributed antenna system structure

where y_i is the received signal at the MS, E is the transmit signal power, h_i denotes the channel fading between DAi and the MS, x is the transmitted symbol from DAi with unit energy, and the entry in the noise z is the complex white Gaussian noise with zero mean and variance N_0.

Composite shadowing/multipath fading environments are frequently encountered in different realistic scenarios. These channels are generally modeled as a mixture of fast fading, path loss, and lognormal shadowing [14]. Therefore, the channel gain h_i in Eq. (1) can be supposed as

$$h_i = g_i \sqrt{P_i(\rho, \theta) S_i} \tag{2}$$

where g_i, $P_i(\rho, \theta)$ and S_i denote the fast fading, path loss and lognormal shadowing, respectively. Furthermore, the three fading effects in Eq. (2) are assumed to be independent of each other. Without loss of generality, the envelope of the fast fading term g_i is assumed to undergo a Rayleigh fading, i.e., the squared envelope $|g_i|^2$ is exponential distributed [15]. For the sake of simplicity, the mean of $|g_i|^2$ is assumed to be unitary, so the PDF of $|g_i|^2$ is as follows

$$f_{|g_i|^2}(t) = \exp(-t), \ t \geq 0. \tag{3}$$

The path loss term $P_i(\rho, \theta)$ in Eq. (2) is a function of the position of MS, which can be modeled as [16]

$$P_i(\rho, \theta) = \left(\frac{d_0}{d_i(\rho, \theta)} \right)^{\beta_i} \tag{4}$$

where d_0 is the reference distance, $d_i(\rho, \theta)$ represents the distance from DAi to the MS located at (ρ, θ), which can be derived as $d_i(\rho, \theta) = \sqrt{\rho^2 + D_i^2 - 2\rho D_i \cos(\theta - \theta_i)}$, and β_i is the path loss exponent. Furthermore, the lognormal shadowing term S_i in Eq. (2) follows a lognormal distribution. For easy analysis, the mean of $10\log_{10} S_i$ is assumed to be zero (in dB). Therefore, the PDF of S_i can be given as [16]

$$f_{S_i}(s) = \frac{\xi}{\sqrt{2\pi}\sigma_i s} \exp\left[-\frac{\left(10\log_{10} s\right)^2}{2\sigma_i^2} \right], \ s > 0 \tag{5}$$

where $\xi = 10/\ln 10$, and σ_i (in dB) is the standard deviation of $10\log_{10} S_i$.

From Eq. (1) and Eq. (2), the received instantaneous output SNR at the MS can be obtained as

$$\gamma_i = \frac{E|h_i|^2}{N_0} = \Omega_i |g_i|^2 \tag{6}$$

where $\Omega_i = EP_i(\rho, \theta) S_i / N_0$. Determined by S_i, Ω_i also follows a lognormal distribution, and its PDF can be expressed as

$$f_{\Omega_i}(\omega) = \frac{\xi}{\sqrt{2\pi}\sigma_i \omega} \exp\left[-\frac{\left(10\log_{10}\omega - \mu_i(\rho, \theta)\right)^2}{2\sigma_i^2} \right], \omega > 0 \tag{7}$$

where $\mu_i(\rho, \theta) = 10\log_{10}(EP_i(\rho, \theta)/N_0)$ is the mean of $10\log_{10}\Omega_i$. Then, from Eq. (3) and Eq. (6), the conditional PDF of γ_i can be derived as [17]

$$f_{\gamma_i|\Omega_i}(\gamma|\omega) = \frac{1}{\omega} \exp\left(-\frac{\gamma}{\omega}\right), \gamma \geq 0. \tag{8}$$

Accordingly, the PDF of γ_i can be obtained from Eq. (7) and Eq. (8) as

$$f_{\gamma_i}(\gamma) = \int_0^{+\infty} \frac{1}{\omega} \exp\left(-\frac{\gamma}{\omega}\right) \frac{\xi}{\sqrt{2\pi}\sigma_i \omega} \exp\left[-\frac{\left(10\log_{10}\omega - \mu_i(\rho,\theta)\right)^2}{2\sigma_i^2}\right] \mathrm{d}\omega \tag{9}$$

It can be observed from Eq. (9) that γ_i follows a gamma-lognormal distribution.

3 Downlink System Capacity Analysis

In this section, the downlink system capacity in DAS will be investigated. For the sake of simplicity, a lognormal distribution is used as an alternative to the gamma-lognormal distribution. Then, using the result, an approximate analytical expression of capacity for the MS over a given position is derived under a selective diversity scheme. Finally, considering the distribution of MSs in the system, a closed-form expression of the system capacity is obtained.

3.1 Approximate Expression of $f_{\gamma_i}(\gamma)$

We can see that the PDF of γ_i in Eq. (9) is a complex integral function, and it's very hard to evaluate it. Referring to [18], the gamma-lognormal distribution in Eq. (9) can be approximated by a lognormal distribution as

$$f_{\gamma_i}(\gamma) \cong \frac{\xi}{\sqrt{2\pi}\tilde{\sigma}_i \gamma} \exp\left[-\frac{\left(10\log_{10}\gamma - \tilde{\mu}_i(\rho,\theta)\right)^2}{2\tilde{\sigma}_i^2}\right], \ \gamma > 0 \tag{10}$$

where $\tilde{\mu}_i(\rho,\theta)$ is the mean of the approximate distribution, which can be achieved as

$$\tilde{\mu}_i(\rho,\theta) = \mu_i(\rho,\theta) - 2.50675 \tag{11}$$

$\tilde{\sigma}_i^2$ in Eq. (10) is the variance of the approximate distribution and can be obtained as

$$\tilde{\sigma}_i^2 = \sigma_i^2 + 31.0215. \tag{12}$$

To verify the impact of using lognormal distribution instead of gamma-lognormal distribution, the accuracy of such approximation is illustrated in Fig. 2. Obviously, the differences between the two distributions are small enough to be ignored.

3.2 Capacity Analysis for the MS Over a Given Position

Assume the channel state information (CSI) between DAi and the MS is known at the transmitter. The selective diversity scheme is applied at the transmitter, i.e., only one distributed antenna is selected for transmission to maximize the output SNR

$$\gamma = \max\{\gamma_0, \gamma_1, \cdots, \gamma_N\}. \tag{13}$$

Owing to the large space among distributed antennas, it is reasonable to assume all the links between distributed antennas and the MS undergo independent shadowing effects and fast fadings, i.e., γ_i in Eq. (13) is independent of γ_j $(i \neq j)$. Then, the cumulative distribution function (CDF) of γ can be obtained as

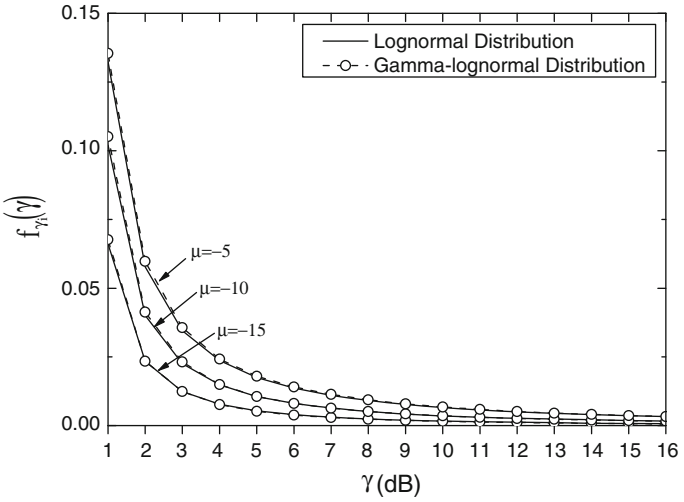

Fig. 2 PDF curves of gamma-lognormal and lognormal distributions

$$F_\gamma(r) = \prod_{i=0}^{N} F_{\gamma_i}(r) = \prod_{i=0}^{N}\left[1 - \frac{1}{2}\mathrm{erfc}\left(\frac{10\log_{10} r - \tilde{\mu}_i(\rho,\theta)}{\sqrt{2}\tilde{\sigma}_i}\right)\right] \tag{14}$$

where $F_{\gamma_i}(r)$ is the CDF of γ_i, and erfc $(\cdot)$ is the complementary error function. The detailed derivation of Eq. (14) can be found in Appendix A. Differentiating Eq. (14) with respect to r yields the PDF of γ as

$$\begin{aligned} f_\gamma(r) &= \sum_{i=0}^{N}\left[f_{\gamma_i}(r)\prod_{j=0,j\neq i}^{N} F_{\gamma_j}(r)\right] \\ &= \sum_{i=0}^{N}\left[\frac{\xi}{\sqrt{2\pi}\tilde{\sigma}_i r}\exp\left(-\frac{\left(10\log_{10} r - \tilde{\mu}_i(\rho,\theta)\right)^2}{2\tilde{\sigma}_i^2}\right)\right. \\ &\quad \left.\times \prod_{j=0,j\neq i}^{N}\left(1 - \frac{1}{2}\mathrm{erfc}\left(\frac{10\log_{10} r - \tilde{\mu}_j(\rho,\theta)}{\sqrt{2}\tilde{\sigma}_j}\right)\right)\right]. \end{aligned} \tag{15}$$

Then, the capacity for the MS located at (ρ, θ) can be derived as

$$\begin{aligned} C(\rho,\theta) &= E_r\left[\log_2(1+r)\right] \\ &= \int_0^{+\infty} \log_2(1+r)\, f_\gamma(r)\mathrm{d}r \\ &= \sum_{i=0}^{N}\int_0^{+\infty} \log_2(1+r)\left[\prod_{j=0,j\neq i}^{N} F_{\gamma_j}(r)\right] f_{\gamma_i}(r)\mathrm{d}r. \end{aligned} \tag{16}$$

Obviously, Eq. (16) is also a complex integral problem, and it's not straight forward to evaluate it. Then, the Gauss-Hermite integral in [19] is applied to approximate Eq. (16) as

$$C(\rho,\theta) \cong \frac{1}{\sqrt{\pi}} \sum_{i=0}^{N} \sum_{n=1}^{N_p} \left\{ H_n \log_2 \left(1 + 10^{\left(\sqrt{2}\tilde{\sigma}_i t_n + \tilde{\mu}_i(\rho,\theta)\right)/10} \right) \times \prod_{j=0, j\neq i}^{N} \left[1 - \frac{1}{2} \mathrm{erfc}\left(\frac{\sqrt{2}\tilde{\sigma}_i t_n + \tilde{\mu}_i(\rho,\theta) - \tilde{\mu}_j(\rho,\theta)}{\sqrt{2}\tilde{\sigma}_j} \right) \right] \right\} \tag{17}$$

where t_n and H_n are the base points and weight factors of the N_p-order Hermite polynomial, respectively. Appendix B gives the detailed derivation of Eq. (17).

3.3 Downlink System Capacity Analysis

Up to now, an approximate expression of downlink capacity is derived in Eq. (17), but this expression is a function of the position of MS, i.e., given a specific position of the MS, a corresponding capacity can be obtained. Theoretically, the system capacity also relates to the distribution of MSs in the cell. Obviously, the expression Eq. (17) doesn't consider the impact of the distribution of MSs on the system capacity. Furthermore, assume that $\delta(\rho,\theta)$ (in polar coordinates) is the PDF that used to describe the distribution of MSs in the cell, and the system capacity can be expressed as

$$\begin{aligned} C_{\text{system}} &= E_{\rho,\theta}\left[C(\rho,\theta)\right] \\ &= \int_0^{2\pi} \int_0^{R} C(\rho,\theta)\,\delta(\rho,\theta)\rho \mathrm{d}\rho \mathrm{d}\theta. \end{aligned} \tag{18}$$

Since the distribution of MSs is arbitrary, the expression in Eq. (18) is complex and usually has no closed-form solution. In this section, by making use of the two-dimensional composite Simpson's rule [20], the final downlink system capacity can be derived as

$$C_{\text{system}} \cong \frac{hk}{9} \sum_{p=0}^{P} \sum_{q=0}^{Q} \left[a_{p,q}\ \rho_p\ C\left(\rho_p,\theta_q\right) \delta\left(\rho_p,\theta_q\right) \right] \tag{19}$$

where the two even numbers P and Q are chosen to determine the step sizes $h = R/P$ and $k = 2\pi/Q$, respectively. In addition, $\rho_p = hp$ and $\theta_q = kq$. The weigh factor $a_{p,q}$ is element of matrix $\mathbf{A}$, in the $(p+1)$ th row and $(q+1)$ th column. Notably, the matrix $\mathbf{A}$ is as follows

$$\mathbf{A} = \begin{bmatrix} 1 & 4 & 2 & 4 & \cdots & 2 & 4 & 1 \\ 4 & 16 & 8 & 16 & \cdots & 8 & 16 & 4 \\ 2 & 8 & 4 & 8 & \cdots & 4 & 8 & 2 \\ \vdots & \vdots & \vdots & \vdots & & \vdots & \vdots & \vdots \\ 4 & 16 & 8 & 16 & \cdots & 8 & 16 & 4 \\ 1 & 4 & 2 & 4 & \cdots & 2 & 4 & 1 \end{bmatrix}_{(P+1)\times(Q+1)} . \tag{20}$$

4 Numerical Results

In this section, both the Monte Carlo simulation results and theoretical results are presented by using the MATLAB simulation tool. The impacts of path loss exponent, number of distributed

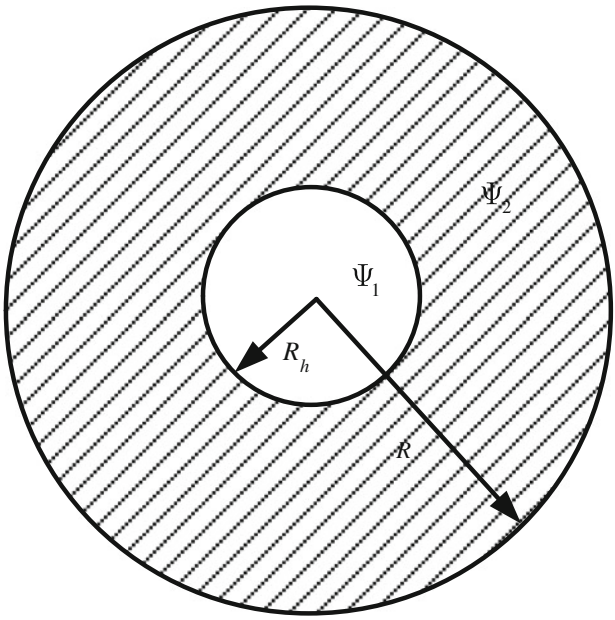

Fig. 3 The distribution of mobile stations in the cell

antennas, as well as the distribution of MSs on the downlink system capacity will be discussed, and the accuracy of system capacity expression will also be verified.

Without loss of generality, a downlink of a single circular DAS is used in this section and the simulation set-up is given as follows. The BS of the system is in the center of the cell, and the distributed antennas are evenly and symmetrically placed in the cell, i.e., the distances between each distributed antenna and the BS are the same, and the angles between every two neighboring DA nodes are also the same. Furthermore, in order to describe the non-uniformity of MSs in the cell, we divide the whole cell into two regions, as shown in Fig. 3. Region 1 (denoted as Ψ_1) is the circular area, which is in the center of the cell and with a radius of R_h. And the residual annular zone is region 2 (denoted as Ψ_2). Therefore, the PDF for describing the distribution of the MSs in the cell can be supposed as

$$\delta(\rho,\theta) = \begin{cases} \dfrac{\lambda}{S_h} & (\rho,\theta) \in \Psi_1 \\ \dfrac{1-\lambda}{S-S_h} & (\rho,\theta) \in \Psi_2 \end{cases} \tag{21}$$

where S_h is the area of region 1, while S is the area of the whole cell. $\lambda \in [0, 1]$ is the probability that MSs distributed in region 1. It can be observed that, the PDF in Eq. (21) varies with the increase or decrease of λ. When $\lambda = S_h/S$, the MSs in the cell follow uniform distribution; when $\lambda > S_h/S$, region 1 is the hot zone, most of the MSs are distributed in this region; when $\lambda < S_h/S$, the majority of MSs are located in region 2. Particularly, the MSs are all distributed in region 2 when $\lambda = 0$, and when $\lambda = 1$, all of MSs are located in region 1. The main parameters used in simulation are listed in Table 1.

Figures 4, 5, 6 and 7 illustrate the downlink system capacity of DAS versus the transmit SNR (E/N_0) in different scenarios. Obviously, it can be found that the performance of system capacity is improved with the increase of E/N_0. Specifically, Figs. 4 and 5 show

Table 1 Main simulation parameters

Parameters	Symbol	Value
Radius of the cell	R	1000 m
Radius of region 1	R_h	250 m
Reference distance	d_0	40 m
Standard deviation of lognormal shadowing	σ_i	8 dB
Order of Hermite polynomial	N_p	40
Number of equidistant nodes for polar radius	P	12
Number of equidistant nodes for polar angle	Q	12
Position of the BS	(D_0, θ_0)	(0, 0)
Positions of DA i, ($i = 1, 2, \cdots, N$)	(D_i, θ_i)	$\left(R/2, 2\pi i/N\right)$

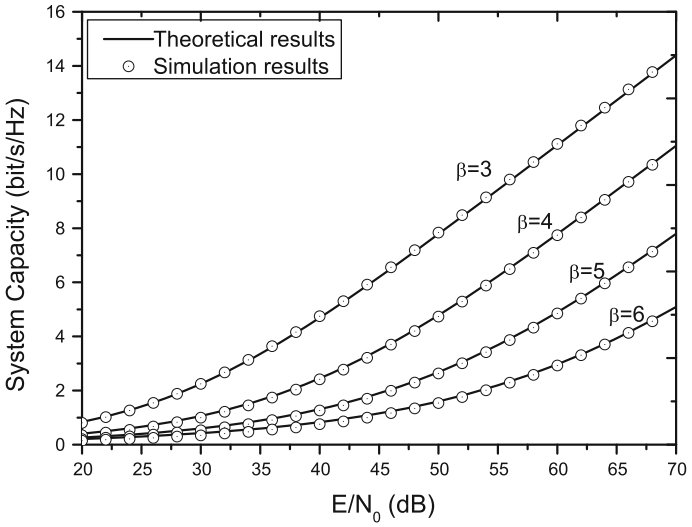

Fig. 4 System capacity versus transmit SNR with different path loss exponents when $\lambda = S_h/S$

the relationship between the system capacity and path loss exponent β when MSs uniformly distributed ($\lambda = S_h/S$) and non-uniformly distributed ($\lambda = 0.4$), respectively. The curves in these two figures indicate that the system capacity value increases with the decrease of path loss exponent. That's because a higher path loss can be achieved with the decrease of the path loss exponent, then a higher output SNR can be obtained, and finally a better capacity performance is derived. Remarkably, the gaps between every two neighboring β enlarge with the increase of E/N_0 , which result in better capacity performances.

Figures 6 and 7 further plot the system capacity as a function of distributed antenna numbers N when MSs uniformly distributed ($\lambda = S_h/S$) and non-uniformly distributed ($\lambda = 0.4$), respectively. Obviously, with the increase of distributed antennas, a higher diversity gain can be achieved, which results in a better output SNR. On the other hand, each MS can obtain a shorter access distance with the increase of distributed antennas, which will make the channel gain larger, and a higher output SNR can also be achieved accordingly.

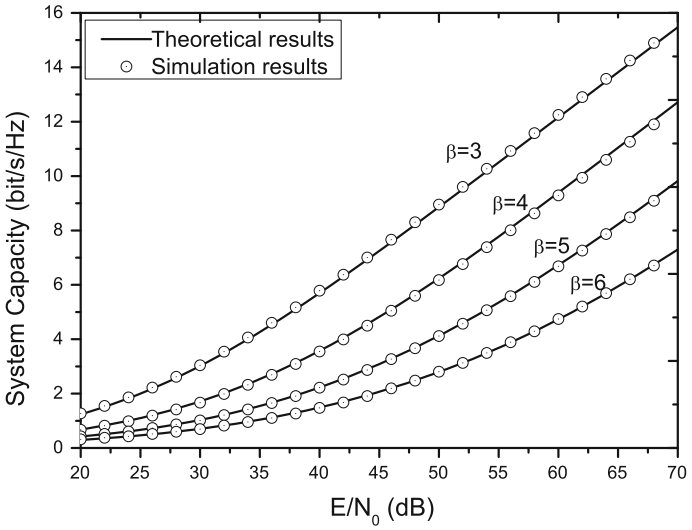

Fig. 5 System capacity versus transmit SNR with different path loss exponents when $\lambda = 0.4$

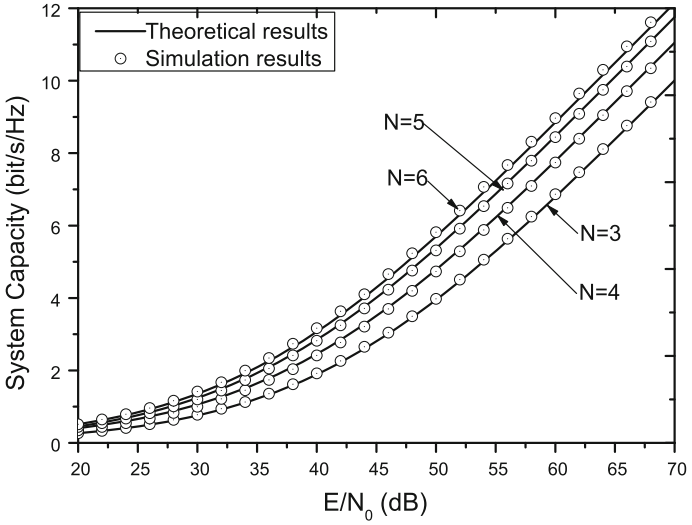

Fig. 6 System capacity versus transmit SNR with different antenna numbers when $\lambda = S_h/S$

As a result, better capacity performances can be obtained with the increase of distributed antennas as shown in these two figures.

It should be emphasized that, from Figs. 4 to 7, the differences between the theoretical results and simulation results are small enough to be ignored, which verifies the accuracy of the theoretical expression of the system capacity. Furthermore, the derived theoretical expression can be employed under different scenarios, and it will lay a good foundation for further research such as network planning and antenna layout in DAS.

Here, we will further compare the system capacity of DAS with the co-located antenna system (CAS) when the MSs are uniformly distributed. In this simulation, the CAS scheme

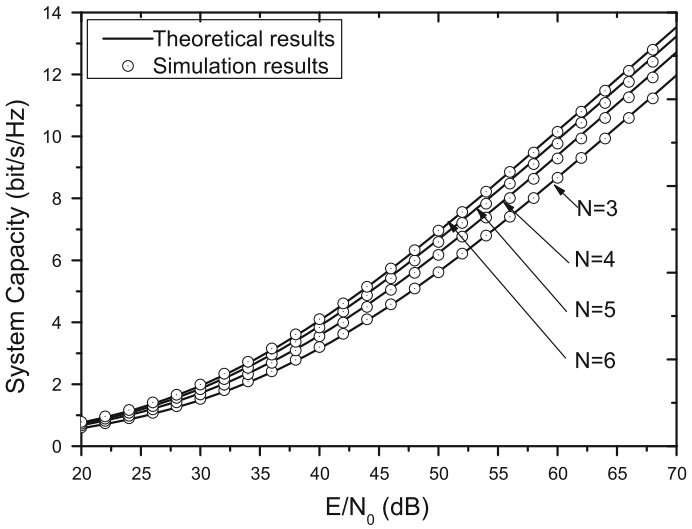

Fig. 7 System capacity versus transmit SNR with different antenna numbers when $\lambda = 0.4$

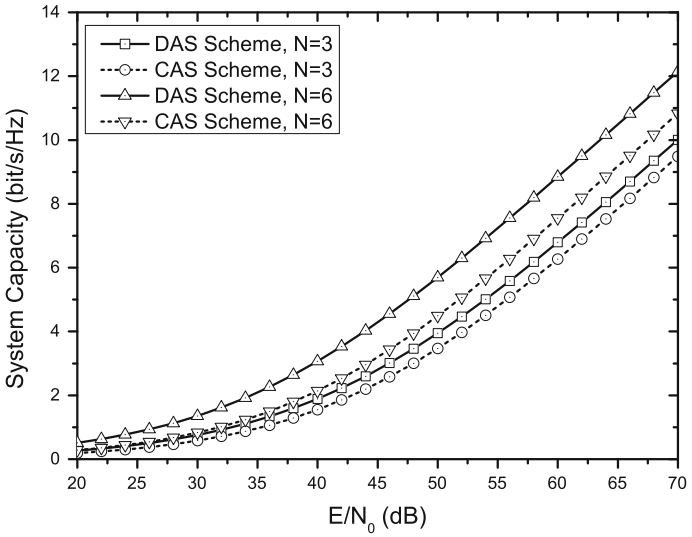

Fig. 8 System capacity comparison between DAS scheme and CAS scheme when MSs are uniformly distributed

employs the same number of antennas as the DAS scheme, and all antennas in CAS scheme are located in the center of the cell. The performance comparison between DAS scheme and CAS scheme can be shown in Fig. 8. It can be observed that, for both the DAS scheme and the CAS scheme, the system capacities are increased with the increase of E/N_0. It should also be noted that the capacity performance of the DAS scheme outperforms the CAS scheme. Moreover, the performance gap between DAS scheme and CAS scheme increases with the increase of antenna numbers.

5 Conclusion

This paper studies the downlink system capacity of DAS with selective diversity scheme. Considering the influence of path loss, lognormal shadowing and Rayleigh fading to the actual wireless environments, this paper firstly establishes a composite channel model. Based on the established composite channel model, an approximate analytical expression of the capacity for a MS over a given position is derived by employing twice approximations. Then, considering the distribution of MSs in the system, a closed-form expression of the system capacity is obtained by using the composite Simpson's rule. Simulation results show that the derived closed-form expression is quite accurate to provide approximations to evaluate the system performance without time-intensive simulations. Moreover, the DAS scheme outperforms the CAS scheme in terms of system capacity when the MSs are uniformly distributed.

Acknowledgments This work is supported by 973 Program of China (2010CB328000), National Nature Science Foundation of China (61102068, 60972023 & 61073168), China Postdoctoral Science Foundation funded project (20110490389), the open research fund of National Mobile Communications Research Laboratory, Southeast University (2010D01), the open research fund of the State Key Laboratory of Integrated Services Networks, Xidian University (ISN12-11), the open research fund of State Key Laboratory of Advanced Optical Communication Systems and Networks (2008SH06), and NUAA Research Funding (NS2011013), National Science and Technology Important Special Project (2010ZX03003-002 & 2010ZX03003-004), and Research Fund of National Mobile Communications Research Laboratory, Southeast University (2011A06).

Appendix A

Due to the independence among γ_i $(i = 0, 1, 2, \cdots, N)$ in Eq. (13), the CDF of output SNR can be obtained as

$$F_{\gamma}(r) = \prod_{i=0}^{N} F_{\gamma_i}(r) \tag{22}$$

where $F_{\gamma_i}(r)$ is the CDF of γ_i . From Eq. (10), $F_{\gamma_i}(r)$ can be expressed as

$$F_{\gamma_i}(r) = \int_0^r \frac{\xi}{\sqrt{2\pi}\tilde{\sigma}_i r} \exp\left[-\frac{\left(10\log_{10} r - \tilde{\mu}_i(\rho,\theta)\right)^2}{2\tilde{\sigma}_i^2}\right] \mathrm{d}r \tag{23}$$

Let $x = \left(10\log_{10} r - \tilde{\mu}_i(\rho,\theta)\right) \Big/ \sqrt{2}\tilde{\sigma}_i$, and substitute x into Eq. (23), $F_{\gamma_i}(r)$ can be further derived as

$$\begin{aligned} F_{\gamma_i}(r) &= \frac{1}{\sqrt{\pi}} \int_{-\infty}^{\frac{10\log_{10} r - \tilde{\mu}_i(\rho,\theta)}{\sqrt{2}\tilde{\sigma}_i}} \exp\left(-x^2\right) \mathrm{d}x \\ &= 1 - \frac{1}{2}\mathrm{erfc}\left(\frac{10\log_{10} r - \tilde{\mu}_i(\rho,\theta)}{\sqrt{2}\tilde{\sigma}_i}\right) \end{aligned} \tag{24}$$

where $\mathrm{erfc}(\alpha) = \left(2/\sqrt{\pi}\right) \int_{\alpha}^{+\infty} \exp\left(-x^2\right) \mathrm{d}x$ is the complementary error function. Then, Eq. (14) is obtained by substituting Eq. (24) into Eq. (22). □

Appendix B

From Eq. (25.4.46) in [19], we can know that the Gauss-Hermite integral formula can be expressed as

$$\int_{-\infty}^{+\infty} f(x) \exp\left(-x^2\right) \mathrm{d}x \cong \sum_{n=1}^{N_p} H_n f(t_n) \tag{25}$$

Let $x = \left(10\log_{10} r - \tilde{\mu}_i(\rho,\theta)\right) \Big/ \sqrt{2}\tilde{\sigma}_i$, and substitute x into Eq. (16), and then using Eq. (25), the expression of capacity for the MS located at (ρ,θ) can be achieved as

$$\begin{aligned} C(\rho,\theta) &= \sum_{i=0}^{N} \frac{1}{\sqrt{\pi}} \int_{-\infty}^{+\infty} \log_2\left(1 + 10^{\left(\sqrt{2}\tilde{\sigma}_i x + \tilde{\mu}_i(\rho,\theta)\right)/10}\right) \\ &\quad \times \left[\prod_{j=0, j\neq i}^{N} F_j\left(10^{\left(\sqrt{2}\tilde{\sigma}_i x + \tilde{\mu}_i(\rho,\theta)\right)/10}\right)\right] \exp\left(-x^2\right) \mathrm{d}x \\ &\cong \frac{1}{\sqrt{\pi}} \sum_{i=0}^{N} \sum_{n=1}^{N_p} \left\{ H_n \log_2\left(1 + 10^{\left(\sqrt{2}\tilde{\sigma}_i t_n + \tilde{\mu}_i(\rho,\theta)\right)/10}\right) \right. \\ &\quad \left. \times \prod_{j=0, j\neq i}^{N} \left[1 - \frac{1}{2}\mathrm{erfc}\left(\frac{\sqrt{2}\tilde{\sigma}_i t_n + \tilde{\mu}_i(\rho,\theta) - \tilde{\mu}_j(\rho,\theta)}{\sqrt{2}\tilde{\sigma}_j}\right)\right]\right\} \end{aligned} \tag{26}$$

Therefore, Eq. (17) is obtained. □

References

1. Dai, L., Zhou, S. D., & Yao, Y. (2005). Capacity analysis in CDMA distributed antenna systems. *IEEE Transactions on Wireless Communications, 4*(6), 2613–2620.
2. Wang, D. M., Wang, X. H., Wang, J. Z., et al. (2008). Spectral efficiency of distributed MIMO cellular systems in a composite fading channel. In *IEEE international conference on communications* (pp. 1259–1264). Piscataway: IEEE.
3. Crisp, M. J., Li, S., & Watts, A. (2007). Uplink and downlink coverage improvements of 802.11g singles using a distributed antenna network. *Journal of Lightwave Technology, 25*(11), 3388–3395.
4. Dai, L. (2008). Distributed antenna system: Performance analysis in multi-user scenario. In *42nd annual conference on inference sciences and systems* (pp. 85–89). Princeton: Computer Society.
5. Castanheira, D., & Gameiro, A. (2010). Distributed antenna system capacity scaling. *IEEE Wireless Communications, 17*(3), 68–75.
6. Shi, C., Wang, Y., Wang, T., et al. (2010). Resource allocation for heterogenerous services per user in OFDM distributed antenna systems. In *IEEE 71st vehicular technology conference.* Taiwan: IEEE
7. You, X. H., Wang, D. M., & Sheng, B., et al. (2010). Cooperative distributed antenna systems for mobile communications. *IEEE Wireless Communications, 17*(3), 35–43.
8. Wang, J. Y., Wang, J. B., Chen, M., et al. (2011). System outage probability analysis of uplink distributed antenna systems over a composite channel. In *IEEE 73rd vehicular technology conference.* Budapest: IEEE.
9. Roh, W., & Paulraj, A. (2002). MIMO channel capacity for the distributed antenna systems. In *IEEE vehicular technology conference* (pp. 706–709). Vancouver: IEEE.
10. Zhuang, H. R., Dai, L., & Xiao, L., et al. (2003). Spectral efficiency of distributed antenna system with random antenna layout. *IEE Electronics Letters, 39*(6), 495–496.

11. Feng, Z. H., Jiang, Z. J., Pan, W., et al. (2008). Capacity analysis of generalized distributed antenna systems using approximation distributions. In *11th IEEE Signapore international conference on communication systems* (pp. 828–830). Piscataway: Computer Society.
12. Chen, H. M., & Chen, M. (2009). Capacity of the distributed antenna systems over shadowed fading channels. In *IEEE 69th vehicular technology conference.* Barcelona: IEEE.
13. Qian, Y. Z., Chen, M., Wang, X. Z., et al. (2009). Antenna location design for distributed antenna systems with selective transmission. In *International conference on wireless communication and signal processing*. Piscataway: IEEE.
14. Li, X., Luo, M. S., Zhao, M., et al. (2009). Downlink performance and capacity of distributed antenna system in multi-user scenario. In *5th International conference on wireless communications. Networking and mobile computing.* Piscataway: Computer Society.
15. McDonough, R. N., & Whalen, A. D. (1995). *Detection of signals in noise* (2nd ed.). California: Academic Press.
16. Goldsmith, A. (2005). *Wireless communication*. New York: Cambridge University Press.
17. Papoulis, A. (1991). *Probability, random variables and statistic processes* (3rd ed.). New York: McGraw-Hill Companies. Inc.
18. Stuber, G. L. (1996). *Principles of mobile communication* (2nd ed.). Dordrecht: Kluwer Academic Publishers.
19. Abramowitz, M., & Stegun, I. A. (1970). *Handbook of mathematical functions with formulas, graphs, and mathematical tables* (9nd ed.). New York: Dover Publications.
20. Burden, R. L., & Faires, J. D. (1989). *Numerical analysis* (4th ed.). Boston: PWS KENT Publishing Company.

Author Biographies

Jun-Bo Wang received his B.S. degree in Computer Science from Hefei University of Technology, Hefei, China, in 2003, and the Ph.D. degree in Electrical Engineering from National Mobile Communications Research Laboratory, Southeast University, China, in 2008. From October of 2008 to April of 2011, he has been a Lecturer at the College of Electronic and Information Engineering, Nanjing University of Aeronautics and Astronautics, Nanjing, China, and from May of 2011 to now he has been an Associate Professor at the college. From March 2011, he has been a postdoctoral research fellow at Key Laboratory for Information System Security of Ministry of Education, School of Software, Tsinghua University, Beijing, China. His current research interests are resource management in wireless communication systems, wireless optical communications and wireless sensor networks.

Jin-Yuan Wang received his B.S. degree in Communication Engineering from College of Information and Electrical Engineering, Shandong University of Science and Technology, Qingdao, China, in 2009. He is currently working toward the M.S. degree at the College of Electronic and Information Engineering, Nanjing University of Aeronautics and Astronautics, Nanjing, China. His research interests include distributed antenna systems and wireless sensor networks.

Ming Chen received his B.Sc., M.Sc. and Ph.D. degrees from mathematics department of Nanjing University, Nanjing, China, in 1990, 1993 and 1996, respectively. In July of 1996, he came to National Mobile Communications Research Laboratory of Southeast University in Nanjing to be a Lecturer. From April of 1998 to March of 2003 he has been an Associate Professor and from April of 2003 to now he has been a Professor at the laboratory. His research interests include signal processing and radio resource management of mobile communication systems.